

## Dephasing of a Superconducting Qubit Induced by Photon Noise

P. Bertet,<sup>1</sup> I. Chiorescu,<sup>1,\*</sup> G. Burkard,<sup>2,3</sup> K. Semba,<sup>1,4</sup> C. J. P. M. Harmans,<sup>1</sup> D. P. DiVincenzo,<sup>2</sup> and J. E. Mooij<sup>1</sup>

<sup>1</sup>Quantum Transport Group, Kavli Institute of Nanoscience, Delft University of Technology, Lorentzweg, Delft, The Netherlands

<sup>2</sup>IBM T. J. Watson Research Center, P.O. Box 218, Yorktown Heights, New York 10598, USA

<sup>3</sup>Department of Physics and Astronomy, University of Basel, Klingelbergstrasse 82, CH-4056 Basel, Switzerland

<sup>4</sup>NTT Basic Research Laboratories, Atsugi-shi, Kanagawa 243-0198, Japan

(Received 19 July 2005; published 13 December 2005)

We have studied the dephasing of a superconducting flux qubit coupled to a dc-SQUID based oscillator. By varying the bias conditions of both circuits we were able to tune their effective coupling strength. This allowed us to measure the effect of such a controllable and well-characterized environment on the qubit coherence. We can quantitatively account for our data with a simple model in which thermal fluctuations of the photon number in the oscillator are the limiting factor. In particular, we observe a strong reduction of the dephasing rate whenever the coupling is tuned to zero. At the optimal point we find a large spin-echo decay time of 4  $\mu$ s.

DOI: 10.1103/PhysRevLett.95.257002

PACS numbers: 74.50.+r, 03.67.Lx, 73.40.Gk

Retaining quantum coherence is a central requirement in quantum information processing. Solid-state qubits, including superconducting ones [1–3], couple to environmental degrees of freedom that potentially lead to dephasing. This dephasing is commonly associated with low-frequency noise [4]. However, resonant modes at higher frequencies are harmful as well. In resonance with the qubit transition they favor energy relaxation. Off resonance they may cause pure dephasing, due to fluctuations of the photon number stored in the oscillator. Experimentally we show that the quantum coherence of our superconducting flux qubit coupled to a dc-SQUID oscillator is limited by the oscillator thermal photon noise. By tuning the qubit and SQUID bias conditions we can suppress the influence of photon noise, and we measure a strong enhancement of the spin-echo decay time from about 100 ns to 4  $\mu$ s.

In our experiment, a flux qubit of energy splitting  $h\nu_q$  is coupled to a harmonic oscillator of frequency  $\nu_p$  which consists of a dc SQUID and a shunt capacitor [5,6]. The oscillator is weakly damped with a rate  $\kappa$  and is detuned from the qubit frequency. In this dispersive regime, the presence of  $n$  photons in the oscillator induces a qubit frequency shift following  $\nu_{q,n} - \nu_{q,0} = n\delta\nu_0$ , where the shift per photon  $\delta\nu_0$  depends on the effective oscillator-qubit coupling. Any fluctuation in  $n$  thus causes dephasing. Taking the oscillator to be thermally excited at a temperature  $T$  and assuming the pure dephasing time  $\tau_\phi \gg 1/\kappa$ , we find [7], after a reasoning similar to [8],

$$\tau_\phi = \frac{\kappa}{\bar{n}(\bar{n} + 1)(2\pi\delta\nu_0)^2} \quad (1)$$

with the average photon number stored in the oscillator  $\bar{n} = [\exp(h\nu_p/kT) - 1]^{-1}$ . We note that a similar effect was observed in a recent experiment on a charge qubit coupled to a slightly detuned waveguide resonator [9]. When driving the oscillator to perform the readout, the authors observed a shift and a broadening of the qubit resonance due to the ac-Stark shift and to photon shot

noise, well-known in atomic cavity quantum electrodynamics [10]. In our experiments, the oscillator is not driven but thermally excited. In addition, we are able to tune *in situ* the coupling constant and  $\delta\nu_0$  and, therefore, to directly monitor the decohering effect of the circuit.

Our flux qubit consists of a micron-size superconducting aluminum loop intersected by four Josephson junctions [11,12] fabricated by standard electron-beam lithography and shadow evaporation techniques [see Fig. 1(a); note that compared to earlier designs [3], we added a fourth junction to restore the qubit-SQUID coupling symmetry [13]]. When the magnetic flux threading the loop  $\Phi_x$  sets the total phase across the junctions  $\gamma_q$  close to  $\pi$ , the loop has two low-energy eigenstates, ground state  $|0\rangle$  and excited state  $|1\rangle$  [3,12]. The flux qubit is characterized by the minimum energy separation  $h\Delta$  between  $|0\rangle$  and  $|1\rangle$ , and the persistent current  $I_p$  [11]. In the basis of the energy eigenstates at the bias point  $\gamma_q = \pi$ , the qubit Hamiltonian reads  $H_q = -(h/2)(\Delta\sigma_z + \epsilon\sigma_x)$ , where  $\epsilon \equiv (I_p/e)(\gamma_q - \pi)/(2\pi)$ . The energy separation is  $E_1 - E_0 \equiv h\nu_q = h\sqrt{\Delta^2 + \epsilon^2}$ . Note that  $d\nu_q/d\epsilon = 0$  when the qubit is biased at  $\epsilon = 0$  so that it is to first order insensitive to noise in  $\epsilon$ , in particular, to noise in the flux  $\Phi_x$ . This is

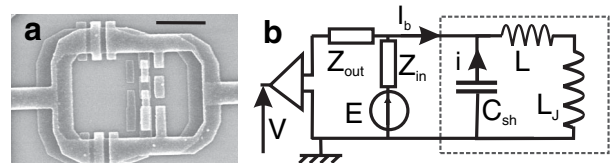


FIG. 1. (a) SEM picture of the sample. The flux qubit is the small loop containing four Josephson junctions in a row; the SQUID is constituted by the outer loop containing the two large junctions. The bar equals 1  $\mu$ m. (b) Measuring circuit diagram. The SQUID, represented by its Josephson inductance  $L_J$ , is shunted by an on-chip capacitor  $C_{sh}$  through superconducting lines of inductance  $L$ , forming the plasma mode.

similar to the doubly optimal point demonstrated in the quantrium experiment [2].

The qubit is inductively coupled to a SQUID detector with a mutual inductance  $M$  [large loop in Fig. 1(a)] and to an on-chip antenna allowing us to apply microwave pulses. The readout scheme and the experimental setup have been described elsewhere [3]. The average persistent current in the qubit loop, with a sign depending on its state  $|k\rangle$  ( $k = 0, 1$ ), generates a flux which modifies its critical current  $I_C \sim 1 \mu\text{A}$  to a value  $I_C^{(k)}$ ; a bias current pulse of amplitude  $I_m$  chosen so that  $I_C^{(0)} < I_m < I_C^{(1)}$  allows us to discriminate between the two states by detecting the switching of the SQUID. Before the measurement, when the bias current  $I_b < I_C$ , the SQUID behaves as a Josephson inductance  $L_J$  which depends on the flux threading it and on  $I_b$ . It is connected to an on-chip capacitor  $C_{\text{sh}}$  through a line with a stray inductance  $L$  [see Fig. 1(b)] and thus forms a harmonic oscillator of frequency  $\nu_p = 1/2\pi\sqrt{(L + L_J)C_{\text{sh}}}$  called the plasma mode [5,6] (note that the junction capacitance is much smaller than  $C_{\text{sh}}$ ). We can write its Hamiltonian  $H_p = \hbar\nu_p a^\dagger a$ , where  $a(a^\dagger)$  is the annihilation (creation) operator. The total current flowing through the SQUID is thus  $I_b + i$ , with  $i = \delta i_0(a + a^\dagger)$  being the operator for the current in the plasma mode and  $\delta i_0$  the rms fluctuations of the current in the oscillator ground state  $\delta i_0 = \sqrt{\hbar\nu_p/2(L + L_J)}$ . The SQUID circuit is connected to the output voltage of our waveform generator  $E$  via an impedance  $Z_{\text{in}}$  and to the input of a room-temperature amplifier through  $Z_{\text{out}}$  which define the oscillator quality factor  $Q = 2\pi\nu_p/\kappa$ .  $Z_{\text{in}}$  and  $Z_{\text{out}}$  take into account low-temperature low-pass filters [3] and on-chip 8 k $\Omega$  thin-film gold resistors thermalized by massive heat sinks. The resulting impedance seen from the plasma mode is estimated to be 9 k $\Omega$  at low frequencies and of order 500  $\Omega$  at GHz frequencies. The measurements were performed at a base temperature  $T_b = 30$  mK.

The applied magnetic field and the bias current  $I_b$  result in a circulating current  $J$  in the SQUID loop [14]. Via the qubit-SQUID coupling  $M$  the qubit phase  $\gamma_q$  will be affected, so that we can write the qubit energy bias as a sum of two contributions  $\epsilon = \eta + \lambda$ , where  $\eta = 2I_p(\Phi_x - \Phi_0/2)/h$  is controlled by  $\Phi_x$  and  $\lambda = 2I_pMJ(I_b)/h$  depends only on  $I_b$  [15]. This dependence has two important consequences. First, the qubit bias point is shifted by the measurement pulse, allowing us to operate the qubit at the flux-noise insensitive point while keeping a measurable signal [3]. Second, it gives rise to a coupling between the qubit and the plasma mode described by a Hamiltonian  $H_I = \hbar[g_1(I_b)(a + a^\dagger) + g_2(I_b)(a + a^\dagger)^2]\sigma_x$ , where  $g_1(I_b) = (1/2)(d\lambda/dI_b)\delta i_0$ , and  $g_2(I_b) = (1/4) \times (d^2\lambda/dI_b^2)(\delta i_0)^2$  [7]. We note that this coupling Hamiltonian depends on  $I_b$  via  $g_1$  and  $g_2$  and is thus tunable *in situ*. In particular it is possible to cancel  $g_1$  by biasing the SQUID at a current  $I_b^*$  such that  $d\lambda/dI_b = 0$ . The qubit is then effectively *decoupled* from its measuring circuit [13].

Our design therefore allows us to study the effect of the coupling between the qubit and its measuring circuit by varying  $I_b$ , while keeping all other parameters unchanged.

To obtain the coupling constants  $g_1$  and  $g_2$ , we performed extensive spectroscopic measurements of the qubit, as a function of both  $I_b$  and  $\Phi_x$ . We applied a prebias current pulse  $I_{bpl}$  through the SQUID while sending a long microwave pulse, followed by a regular measurement pulse [3] at a value  $I_m$  [see Fig. 2(a)]. We measured the SQUID switching probability as a function of the microwave frequency and recorded the position of the qubit resonance as a function of  $I_{bpl}$  and  $\Phi_x$ . The data are shown in Fig. 2(a) for various values of  $I_{bpl}$ . We observe that for each bias current, a specific value of external flux  $\Phi_x^0(I_{bpl})$  realizes the optimal point condition. Fitting all the curves with the formula  $\nu_q = \sqrt{\Delta^2 + [\lambda(I_{bpl}) + 2I_p(\Phi_x - \Phi_0/2)/h]^2}$ , we obtain the qubit parameters  $M = 6.5$  pH,  $\Delta = 5.5$  GHz,  $I_p = 240$  nA, and also  $\lambda(I_b)$  which is shown in Fig. 2(b) together with a parabolic fit. Decoupling occurs at  $I_b^* = 180 \pm 20$  nA and not at  $I_b = 0$  because of a 4% asymmetry of the SQUID junctions. We also measured the parameters of the SQUID oscillator by performing resonant activation measurements and fitting the dependence of the resonant activation peak as a function of  $I_b$  and  $\Phi_x$  [6]. We found a maximum plasma frequency  $\nu_p = 3.17$  GHz,  $C_{\text{sh}} = 7.5 \pm 2$  pF, and  $L = 100 \pm 20$  pH, consistent with design values. The width of the peak also

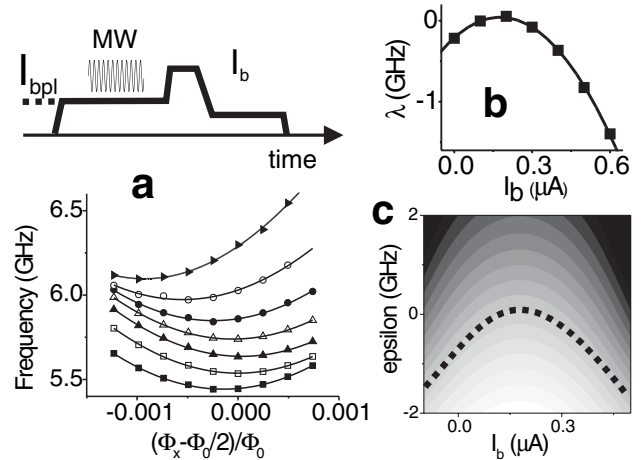


FIG. 2. (a) Top: principle of the spectroscopy experiments: a bias current pulse of amplitude  $I_{bpl} < I_C \sim 1 \mu\text{A}$  is applied while a microwave pulse (MW) probes the qubit resonance frequency. The qubit state is finally measured by a short bias current pulse as discussed in Ref. [3]. Bottom: Qubit spectroscopy for  $I_{bpl}$  varying between 0 and  $0.6 \mu\text{A}$  with steps of  $0.1 \mu\text{A}$  (bottom to top). The curves were offset by 100 MHz for clarity. The solid curves are fits to the formula for  $\nu_q$ . (b) Curve  $\lambda(I_b)$  deduced from the spectroscopy curves as explained in the text. The solid line is a parabolic fit to the data. The decoupling condition is satisfied at  $I_b^* = 180 \pm 20$  nA. (c) Calculated frequency shift  $\delta\nu_0(I_b, \epsilon)$  for the parameters of our sample. The white scale corresponds to  $-20$  MHz, the black to  $+40$  MHz. Along the dotted line  $\epsilon_m(I_b)$ ,  $\delta\nu_0 = 0$ .

gives us an estimate for the oscillator quality factor,  $Q = 120 \pm 30$ .

From the previous measurements we know the parameters of the total Hamiltonian  $H = H_q + H_p + H_I$  and we can deduce the value of  $\delta\nu_0$  by second-order perturbation theory [7]:  $\delta\nu_0 = 4[[g_1(I_b)\sin\theta]^2 \frac{\nu_q}{\nu_q - \nu_p} - g_2(I_b)\cos\theta]$ , where  $\theta$  is the mixing angle, defined by  $\cos\theta = \epsilon/\sqrt{\epsilon^2 + \Delta^2}$ . The first term in  $\delta\nu_0$  is the usual ac-Zeeman shift obtained without using the rotating wave approximation which is not valid in our case. Note, in particular, that the sign of this shift depends only on the sign of  $\nu_q - \nu_p$  which in our experiments is always positive. The second term is due to the dependence of the SQUID Josephson inductance on the qubit state [6,16], and it has the same sign as  $\epsilon$  since  $g_2$  is negative. Therefore, for some value  $\epsilon_m(I_b) < 0$ , one obtains  $\delta\nu_0 = 0$ . This is shown as a dashed line in Fig. 2(c) in which we plot  $\delta\nu_0(\epsilon, I_b)$ . If dephasing is indeed limited by thermal fluctuations, we expect the dephasing time to be maximal along  $\epsilon_m(I_b)$ . We note that the curve includes  $(I_b = I_b^*, \epsilon = 0)$ , so that this bias point is *optimal* with regard to bias current noise, flux noise, and photon noise.

We now turn to the measurements of the qubit coherence properties around this optimal point, as characterized by the relaxation time  $T_1$ , the qubit spectral line shape, and the spin-echo decay time  $T_{\text{echo}}$  [17]. The line shape was measured using a long microwave pulse (2  $\mu\text{s}$ ) at a power well below saturation. Figure 3(a) shows a typical result at the optimal point. For this specific sample, we observed a twin peak structure which likely results from one strongly coupled microscopic fluctuator. In addition, the width of the line as well as the average value of the gap  $\Delta$  changed significantly in time, which indicates that the residual linewidth is probably due to a larger number of fluctuators more weakly coupled. We stress that we observed the splitting all along the  $\nu_q(\Phi_x)$  spectrum in contrast to Ref. [18]. Fitting the peaks to a sum of two Lorentzians of widths  $w_1$  and  $w_2$  we define an effective dephasing time  $t_2 = 2/\pi(w_1 + w_2)$ . At the optimal point  $t_2$  varied between 50 and 200 ns.

Despite the fluctuators, we were able to induce Rabi oscillations by applying microwave pulses at the middle frequency of the split line. An example is shown in Fig. 3(b) at the optimal point. The oscillations decay non-exponentially and display a clear beating. Nevertheless, by driving the qubit strongly enough, we could observe well-behaved oscillations for hundreds of nanoseconds [see the inset of Fig. 3(b)]. We measured the energy relaxation time  $T_1$  by applying a  $\pi$  pulse followed after a delay  $Dt$  by a measurement pulse [see Fig. 3(c)]. At the optimal point, we found that  $T_1 = 4 \mu\text{s}$ . To quantify the dephasing further we also applied the spin-echo sequence [17], depicted in Fig. 4(a). Spin-echo measurements are particularly relevant for our purpose, because the photon noise in the plasma mode occurs at a relatively high frequency set by  $\kappa \approx 130 \text{ MHz}$ . In such conditions, this noise affects the

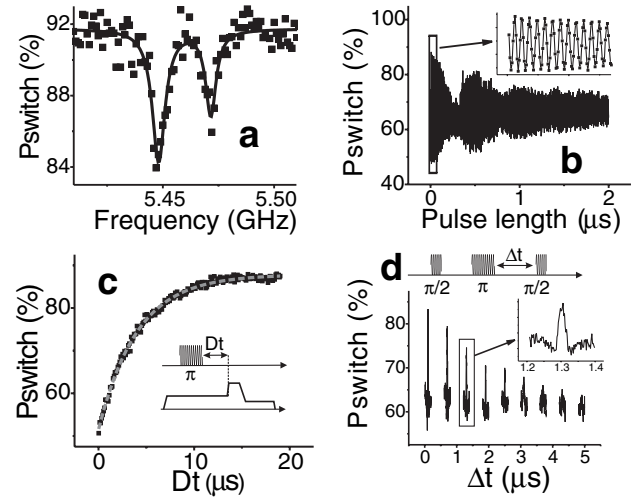


FIG. 3. (a) Qubit line shape at the optimal point. The solid line is a fit assuming a double Lorentzian shape. (b) Rabi oscillations (frequency 100 MHz) at the optimal point. The inset shows well-behaved oscillations with nearly no damping during the first 100 ns. (c) Measurement of  $T_1$  at the optimal point; the dashed gray line is an exponential fit of a time constant 4  $\mu\text{s}$ . (d) Spin-echo pulse sequence and signal at the optimal point.

spin-echo damping time  $T_{\text{echo}}$  as strongly as Ramsey experiments so that  $T_{\text{echo}}$  is also given by formula (1) [7]; on the other hand, the spin-echo experiment is not sensitive to the low-frequency noise responsible for the qubit line splitting. The results are shown in Fig. 3(d) at the optimal point, by a set of curves obtained at different delays  $\Delta t$  between the  $\pi$  pulse and the last  $\pi/2$  pulses. Fitting the decay of the echo amplitude as a function of the delay between the two  $\pi/2$  pulses with an exponential, we find  $T_{\text{echo}} = 3.9 \pm 0.1 \mu\text{s}$ . Compared with previous experiments on flux qubits [3], the long Rabi and spin-echo times were obtained by reducing the mutual inductance  $M$ , and biasing the qubit at the optimal point.

We studied the variation of  $T_1$  as a function of the bias current at the flux-insensitive point  $\epsilon = 0$ . This required us to adjust the flux at the value  $\Phi_x(I_b)$ . Results are shown in Fig. 4(a). We observed a clear maximum of  $T_1$  for  $I_b = I_b^*$ . This demonstrates that at least part of the qubit relaxation occurs by dissipation in the measuring circuit. We then investigated the dependence of  $T_{\text{echo}}$  and  $t_2$  on  $\epsilon$  for  $I_b = I_b^*$  [Fig. 4(b) top, circles and squares]. As expected, we observe a sharp maximum for  $T_{\text{echo}}$  at  $\epsilon = 0$  and a shallow one for  $t_2$ . However, at a different bias current  $I_b = 0 \mu\text{A}$ , the maximum of  $T_{\text{echo}}$  and  $t_2$  is clearly shifted towards  $\epsilon < 0$ . We measured the position of this maximum in  $t_2$  as a function of  $I_b$  as shown by the squares in Fig. 4(c). For dephasing caused by flux noise or bias current noise, the maximal coherence time should always be obtained at  $\epsilon = 0$ ; the observed deviation proves that a different noise source is active in our experiments. We find that thermally induced photon number fluctuations in the plasma mode explains our results. In Fig. 4(c) we draw the curve  $\epsilon_m(I_b)$  of Fig. 2(c), where the photon-induced shift  $\delta\nu_0$  equals 0

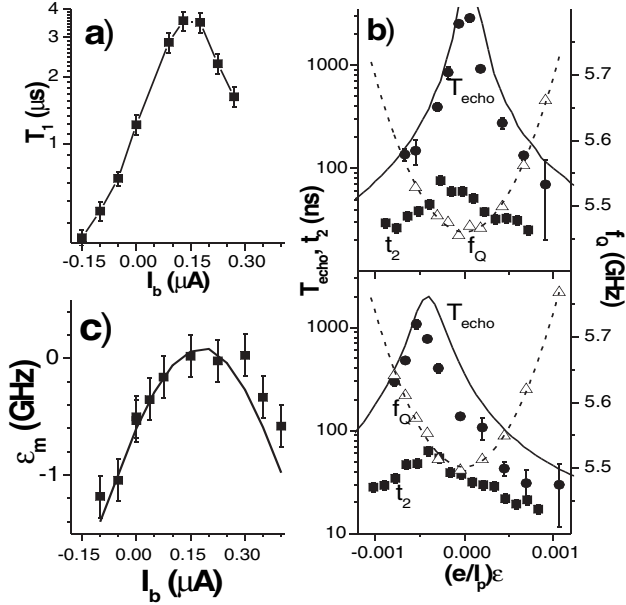


FIG. 4. (a) Measurement of  $T_1$  versus  $I_b$  at the flux-noise insensitive point  $\epsilon = 0$ . (b) Measurement of  $T_{\text{echo}}$  (circles),  $t_2$  (squares), and of the qubit frequency (triangles), as a function of  $\epsilon$  for  $I_b = I_b^*$  (top) and  $I_b = 0 \mu\text{A}$  (bottom). The dotted line is a fit to the formula for  $\nu_q$ ; the solid black line is the prediction of Eq. (1) for  $T = 70 \text{ mK}$  and  $Q = 150$ . (c) Value of  $\epsilon$  for which  $t_2$  is maximum (full squares) compared to the theoretical  $\epsilon_m(I_b)$  (full line).

(solid line). The agreement between the data points and this curve, obtained directly from measured parameters, is excellent. In addition, assuming a reasonable effective oscillator temperature of  $T = 70 \text{ mK}$  [5] and a quality factor of  $Q = 150$ , which yields a mean photon number  $\bar{n} = 0.15$ , the dephasing time  $\tau_\phi$  predicted by Eq. (1) closely matches the spin-echo measurements both for  $I_b = I_b^*$  and  $I_b = 0 \mu\text{A}$  [19] [see the solid line in Fig. 4(b)]. We stress that even at such small  $\bar{n}$  the photon number fluctuations can strongly limit the qubit coherence. This suggests that increasing the plasma frequency could lead to significant improvement.

In conclusion, we present experimental evidence that the dephasing times measured in a flux qubit can be limited by thermal fluctuations of the photon number in the SQUID detector plasma mode to which it is strongly coupled. By careful tuning of flux and current bias, we could decouple the qubit from its detector and reach long relaxation and spin-echo damping times ( $4 \mu\text{s}$ ). These results indicate that long coherence times can be achieved with flux qubits.

We thank Y. Nakamura, D. Estève, D. Vion, M. Grifoni for fruitful discussions. This work was supported by the Dutch Foundation for Fundamental Research on Matter (FOM), the E. U. Marie Curie and SQUBIT grants, and the U.S. Army Research Office.

\*Present address: National High Magnetic Field Laboratory, Florida State University, 1800 East Paul Dirac Drive, Tallahassee, FL 32310, USA.

- [1] Y. Nakamura, Yu. A. Pashkin, and J. S. Tsai, *Nature (London)* **398**, 786 (1999); J. M. Martinis, S. Nam, J. Aumentado, and C. Urbina, *Phys. Rev. Lett.* **89**, 117901 (2002); T. Duty, D. Gunnarsson, K. Bladh, and P. Delsing, *Phys. Rev. B* **69**, 140503 (2004); J. Claudon, F. Balestro, F. W. Hekking, and O. Buisson, *Phys. Rev. Lett.* **93**, 187003 (2004).
- [2] D. Vion, A. Aassime, A. Cottet, P. Joyez, H. Pothier, C. Urbina, D. Estève, and M. H. Devoret, *Science* **296**, 886 (2002).
- [3] I. Chiorescu, Y. Nakamura, C. J. P. M. Harmans, and J. E. Mooij, *Science* **299**, 1869 (2003).
- [4] E. Paladino, L. Faoro, G. Falci, and R. Fazio, *Phys. Rev. Lett.* **88**, 228304 (2002); Y. Makhlin and A. Shnirman, *Phys. Rev. Lett.* **92**, 178301 (2004).
- [5] I. Chiorescu, P. Bertet, K. Semba, Y. Nakamura, C. J. P. M. Harmans, and J. E. Mooij, *Nature (London)* **431**, 159 (2004).
- [6] P. Bertet, I. Chiorescu, K. Semba, C. J. P. M. Harmans, and J. E. Mooij, *Phys. Rev. B* **70**, 100501 (2004).
- [7] P. Bertet, I. Chiorescu, C. J. P. M. Harmans, and J. E. Mooij, *cond-mat/0507290*.
- [8] A. Blais, R.-S. Huang, A. Wallraff, S. M. Girvin, and R. J. Schoelkopf, *Phys. Rev. A* **69**, 062320 (2004).
- [9] D. I. Schuster, A. Wallraff, A. Blais, L. Frunzio, R.-S. Huang, J. Majer, S. M. Girvin, and R. L. Schoelkopf, *Phys. Rev. Lett.* **94**, 123602 (2005).
- [10] M. Brune, E. Hagley, J. Dreyer, X. Maître, A. Maali, C. Wunderlich, J. M. Raimond, and S. Haroche, *Phys. Rev. Lett.* **77**, 4887 (1996).
- [11] J. E. Mooij, T. P. Orlando, L. Levitov, L. Tian, C. H. van der Wal, and S. Lloyd, *Science* **285**, 1036 (1999).
- [12] C. H. van der Wal, A. C. J. ter Haar, F. K. Wilhelm, R. N. Schouten, C. J. P. M. Harmans, T. P. Orlando, S. Lloyd, and J. E. Mooij, *Science* **290**, 773 (2000).
- [13] G. Burkard, D. P. DiVincenzo, P. Bertet, I. Chiorescu, and J. E. Mooij, *Phys. Rev. B* **71**, 134504 (2005).
- [14] V. Lefèvre-Seguin, E. Turlot, C. Urbina, D. Estève, and M. H. Devoret, *Phys. Rev. B* **46**, 5507 (1992).
- [15] In the conditions of our experiments, we can safely neglect the additional dependence of  $J$  and thus  $\lambda$  on  $\Phi_x$ .
- [16] A. Lupascu, C. J. M. Verwijs, R. N. Schouten, C. J. P. M. Harmans, and J. E. Mooij, *Phys. Rev. Lett.* **93**, 177006 (2004).
- [17] Y. Nakamura, Y. A. Pashkin, T. Yamamoto, and J.-S. Tsai, *Phys. Rev. Lett.* **88**, 047901 (2002); E. Collin, G. Ithier, A. Aassime, P. Joyez, D. Vion, and D. Estève, *Phys. Rev. Lett.* **93**, 157005 (2004).
- [18] R. W. Simmonds, K. M. Lang, D. A. Hite, S. Nam, D. Pappas, and J. M. Martinis, *Phys. Rev. Lett.* **93**, 077003 (2004).
- [19] We actually plot  $[\tau_\phi^{-1} + (2T_1)^{-1}]^{-1}$ , where  $T_1$  is the value measured at each bias current ( $T_1 = 4 \mu\text{s}$  for  $I_b = I_b^*$ , and  $T_1 = 1 \mu\text{s}$  for  $I_b = 0 \mu\text{A}$ ).